

Tropospheric Delay Estimation Based on Numerical Weather Model

Constantin-Octavian ANDREI, Finnish Geodetic Institute, octavian.andrei@fgi.fi

Chen RUIZHI, Finnish Geodetic Institute, ruizhi.chen@fgi.fi

***Summary:** This paper describes an algorithm for estimating the tropospheric delay based on the Numerical Weather Model and its implementation using an object-oriented approach. The Global Data Assimilation System model used in the investigation is produced by the National Centers for Environmental Prediction of the US National Oceanic and Atmospheric Administration. Using the GDAS model, atmospheric parameters such as pressure, temperature and relative humidity are extracted and then used in a standard tropospheric model. The Saastamoinen Model is used in this paper for computing zenith delays, and together with Ifadis mapping function to convert zenith delays into slant path delays. The entire algorithm assumes as input data the location of a given point and the time, while the output values are the hydrostatic and wet components of the total tropospheric zenith delay. The obtained results were compared with International GNSS Service tropospheric delays.*

1. Introduction

The Earth's atmosphere is consisted of dry gases and water vapour. The wet and dry constituents of the atmosphere affect the propagation of GPS signals, specially, in the lowest parts of the Earth's atmosphere such as the ionosphere and the neural atmosphere. Normally, global atmospheric models are used to correct for the atmospheric effect in most of GPS applications with modest accuracy demands. However, for high accuracy GPS applications, the global models are not sufficiently accurate and other measures have to be included in the data processing in order to handle the atmospheric effects.

The ionosphere is the dominant source of error being frequency-dependent. As a consequence, its effect is commonly mitigated using dual-frequency receivers, although this is not the case for single-frequency receivers [Le, 2007]. The neural atmosphere (the troposphere and the stratosphere) is another major source of error in GPS satellite based applications. The effect caused by the neural atmosphere, normally referred as the tropospheric delay [Hofmann-Wellenhof, 2004], is handled using global tropospheric delays models where meteorological measurements are available to help quantify the state of the neutral atmosphere.

For most of the post-processing GPS applications, the positioning is based on long time observation. In this case, the considerable amount of used data leaves enough degree of freedom in the adjustment post-processing to estimate the residual tropospheric effect as a separate parameter in the adjustment. This approach is used for instance by the Bernese GPS Data Processing software [Jensen, 2002]. On the other hand, for real time GPS applications the amount of data is not enough to estimate the size of the residual tropospheric error. Therefore, other methods for estimating the residual tropospheric effect must be used. One way to overcome this problem is to use the potential of the Numerical Weather Model (NWM) as it is described in this paper.

2. Tropospheric Delay

The signal received from a GPS satellite is refracted by the atmosphere as it travels to the user on the layer near the Earth's surface. The atmospheric refraction causes a delay that depends upon the actual path of the ray and the refractive index of the gases along that path. There are two

major delay effects of the troposphere: the dry or hydrostatic tropospheric delay and the wet or non-hydrostatic tropospheric delay.

Following Hofmann-Wellenhof (2004), the tropospheric path delay is defined as the difference between actual ray path and the geometrical:

$$\Delta^{Trop} = \int n ds - \int ds = \int (n - 1) ds \quad (1)$$

with n denoting the refractive index.

Usually, instead of the refractive index n the refractivity

$$N^{Trop} = 10^6 (n - 1) \quad (2)$$

is used so that Eq.(1) becomes:

$$\Delta^{Trop} = 10^{-6} \int N^{Trop} ds \quad (3)$$

The refractivity can be determined using the expression below from Langley (1996):

$$N = k_1 \frac{P_d}{T} Z_d^{-1} + \left(k_2 \frac{e}{T} + k_3 \frac{e}{T^2} \right) Z_w^{-1} \quad (4)$$

where the dry part is denoted by subscript d , and subscript w denotes the wet part, k_1, k_2 and k_3 are constants, P_d is the partial pressure of the dry air, T temperature and e is the partial pressure of water vapour, Z_d and Z_w are the compressibility factors for dry air and water vapour respectively. The first term of Eq.(4) is called the dry refractivity, since it depends only on the dry constituents. The term in the last bracket is correspondently called wet refractivity. Alternatively, the terms hydrostatic and non-hydrostatic refractivity are also found in the literature. However, the former ones are used in this paper.

The total tropospheric delay, Δ^{Trop} , can now be determined as:

$$\Delta^{Trop} = 10^{-6} \int N_d ds + 10^{-6} \int N_w ds \quad (5)$$

The dry component of the tropospheric delay is about 90% of the total delay, corresponds to approximately 2.3 m in the zenith direction and varies with the local temperature and atmospheric pressure [Spilker, 1996]. The wet component is generally smaller, from a few mm in dry arctic areas or in deserts to 40 cm in tropical regions, and less predictable even with surface measurements [Brunner and Welsch, 1993].

3. Numerical Weather Model

The Numerical Weather Models are three dimensional models of the atmospheric conditions in the lowest part of the atmosphere, from the surface of the Earth up to an altitude of about 30 km. The models contain predicted information about different meteorological parameters such as temperature, relative humidity, geopotential height, and two horizontal wind components. The purpose of the NWM is to predict the future state of the atmospheric circulation from the information on the present conditions by using numerical approximations of the dynamical equations describing the atmospheric circulation [Holton, 1992].

3.1. GDAS model

The GDAS (Global Data Assimilation System) model used for this study is produced by the National Centers for Environmental Prediction (NCEP) of the US National Oceanic and Atmospheric Administration (NOAA) and shown in Fig. 1. The output data have a temporal resolution of 6 hours with 3 h forecast cycles. This means that a final analysis takes place four times per day, i.e., at 00, 06, 12 and 18 UTC and serves as basis for predictions in 3 h intervals. The output data has a horizontal resolution of $1^\circ \times 1^\circ$ and a vertical resolution of 23 pressure layers up to 20 hPa. The GDAS weather fields contain 35 different quantities, but the most interesting for this

study were geopotential height (23 layers, between 1000 ... 10 hPa), temperature (23 layers, same pressure levels as for geopotential height) and relative humidity (21 layers same as pressure levels, except the last two of 50 and 20 hPa).

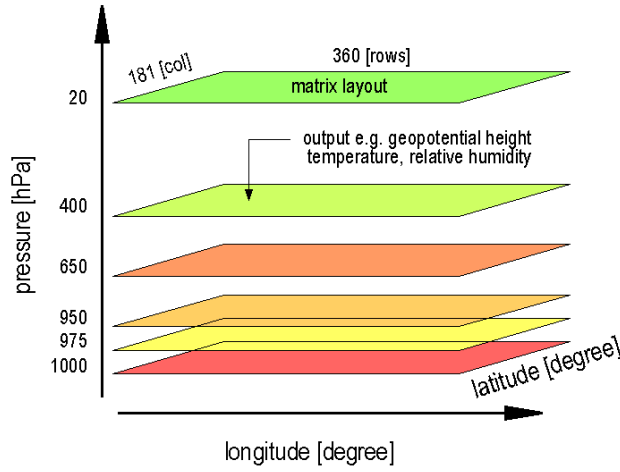


Fig. 1: Data representation in the global Numerical Weather Model

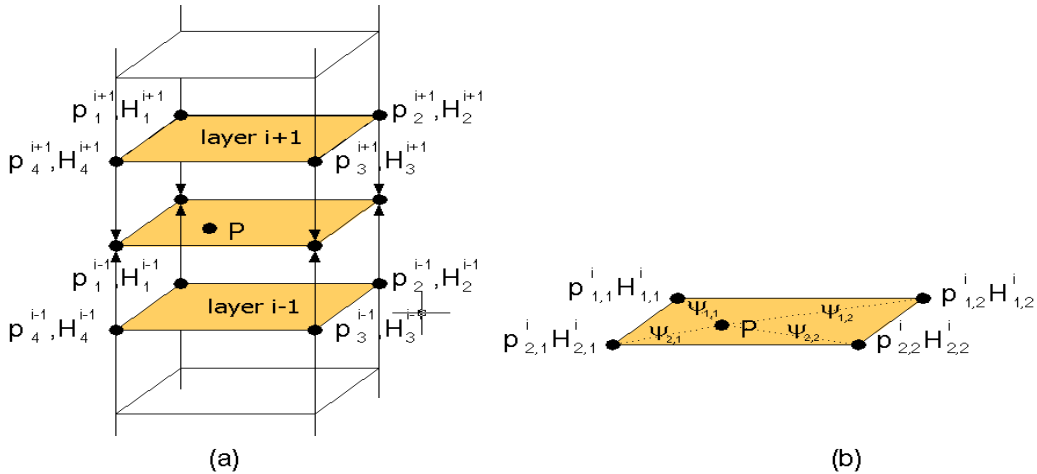


Fig. 2: Vertical (a) and horizontal (b) interpolation in NWM data extraction strategy.

3.2. Data extraction strategy

Many troposphere models need meteorological information at the observation height as input, with pressure being of an essential parameter for determination of wet zenith delays. The accuracy requirement is in the range of 0.5 hPa to a maximum of 1 hPa corresponding to roughly 1.5 to 3 mm error in Δ_w^{Trop} .

Schueler (2001) analyzed different approaches to extract meteorological data from a NWM. In brief, three main steps for data extraction were carried out:

- Vertical interpolation (Figure 2a) is performed with respect to observation height for all four nearest neighbouring horizontal grid points of the weather field. Pressure data are interpolated by exponential function, while temperature and relative humidity are obtained by linear interpolation.
- Horizontal interpolation (Figure 2b) is performed with all four neighbouring points using normalized weights defined by the reciprocal spherical distance between target and grid point raised to the weighting power c (here 1.5 was chosen).
- Interpolation in time domain is performed using either linear functions or cubic splines.

4. Tropospheric Delay Modelling

In GPS applications, the tropospheric delay is handled by means of global tropospheric delay models based on climate data. Some models are explicitly dependent on surface meteorological data and others use the coordinates (latitude and height) of the GPS station.

4.1. The Saastamoinen Model

Saastamoinen (1973) developed both a precise model and a simpler standard model. The standard model, which is given below, is widely used in GPS applications and is a three-parameter model:

$$\Delta^{Trop} = 0.002277 \cdot \left[P + \left(\frac{1255}{T} + 0.05 \right) \cdot e \right] \quad (6)$$

where P is the surface atmospheric pressure in mbar, T is the surface temperature in Kelvin, e is the surface partial pressure of water vapor in mbar.

Mendes and Langley (1998) assessed a various number of zenith delay prediction models using a one-year data set of radiosonde profiles from 50 stations distributed worldwide. The results of their assessment are the following. The Saastamoinen had outstanding performance with submillimeter bias and RMS scatter for hydrostatic zenith delay with respect to the benchmark values. Saastamoinen was ranked among the best for wet zenith delay, and had a better match with radiosonde ray tracing results, less than 1 cm of bias and a few centimeters of RMS scatter for total zenith delay. Conversely, the Hopfield model, which also uses P, T, e at the observation location as input, tends to over-predict the zenith delay except for the equatorial region.

4.2. Ifadis mapping function

The total tropospheric delay for a satellite signal received at any elevation angle can be estimated, by first, determining the zenith delay and then multiplying the zenith delay with a unitless mapping factor. The factor is determined by a mapping function, $m(E)$, and often both a hydrostatic and a wet mapping function is used, so that the total delay at any elevation, E , is determined as:

$$\Delta^{Trop} = \Delta_d^{Trop} \cdot m_d(E) + \Delta_w^{Trop} \cdot m_w(E) \quad (7)$$

where Δ_d^{Trop} is the zenith dry delay, Δ_w^{Trop} is the zenith wet delay, $m_d(E)$ and $m_w(E)$ are the dry and wet mapping functions that magnify the tropospheric delay as the elevation angle E decreases. The mapping factor is about 4 for a 15° elevation angle, about 6 for a 10° elevation angle, and about 10 for a 5° elevation angle.

Several mapping functions have been developed during the last decades such as Ifadis (1986), Herring (1992), Niell (1996). They use the following type of the mapping function that is elevation angle dependent:

$$M(E) = \frac{1 + \frac{a}{1 + \frac{b}{1 + c}}}{\sin E + \frac{a}{\sin E + \frac{b}{\sin E + c}}} \quad (8)$$

Apart from different representations, the mapping functions differ in parameterization of the coefficients a, b , and c . Since these parameters depend on the quotient of the scale height and the

radius of the earth, best fits are to be found from either standard profiles or profiles from radiosonde data [Kleijer, 2004].

Mendes (1999) analyzed 12 different mapping functions, using the same radiosonde data as for the zenith delay tests mentioned before. He concluded that the Niell mapping function (NMF) [Niell, 1996] is the overall best mapping function when no meteorological data is available. If meteorological observations are available, the Ifadis and MTT [Herring, 1992] mapping function are recommended.

In 1992, Ifadis investigated real weather profiles from various sites distributed over large areas of the world and with different climatic conditions. For most of the stations, Ifadis had a three-year database in the period 1978-1984. Using a ray-tracing algorithm, he developed a global hydrostatic mapping function that can be used down to 2° elevation angle, and determined the following constants:

$$\begin{aligned} a &= 0.1237 \cdot 10^{-2} + 0.1316 \cdot 10^{-6}(P - 1000) + 0.1378 \cdot 10^{-5}(t - 15) + 0.8057 \cdot 10^{-5} \sqrt{e} \\ a &= 0.3333 \cdot 10^{-2} + 0.1946 \cdot 10^{-6}(P - 1000) + 0.1040 \cdot 10^{-6}(t - 15) + 0.1747 \cdot 10^{-4} \sqrt{e} \quad (9) \\ c &= 0.078 \end{aligned}$$

The non-hydrostatic mapping function has the constants [Mendes, 1999]:

$$\begin{aligned} a &= 0.5236 \cdot 10^{-3} + 0.2471 \cdot 10^{-6}(P - 1000) - 0.1724 \cdot 10^{-6}(t - 15) + 0.1328 \cdot 10^{-4} \sqrt{e} \\ a &= 0.1705 \cdot 10^{-2} + 0.7348 \cdot 10^{-6}(P - 1000) + 0.3767 \cdot 10^{-6}(t - 15) + 0.2147 \cdot 10^{-4} \sqrt{e} \quad (10) \\ c &= 0.05917 \end{aligned}$$

with P total surface pressure in mbar, e surface partial pressure of water vapour in mbar, and t surface temperature in Celsius.

In this paper, instead of applying default meteorological values of the standard atmosphere, more realistic temperature, pressure and partial pressure vapour water values are extracted from the GDAS and then used in a tropospheric model. The Ifadis mapping function is used together with the Saastamoinen model.

5. Implementation

The entire algorithm was implemented using an object-oriented approach in C++ programming language and the main steps are presented in Figure 3.

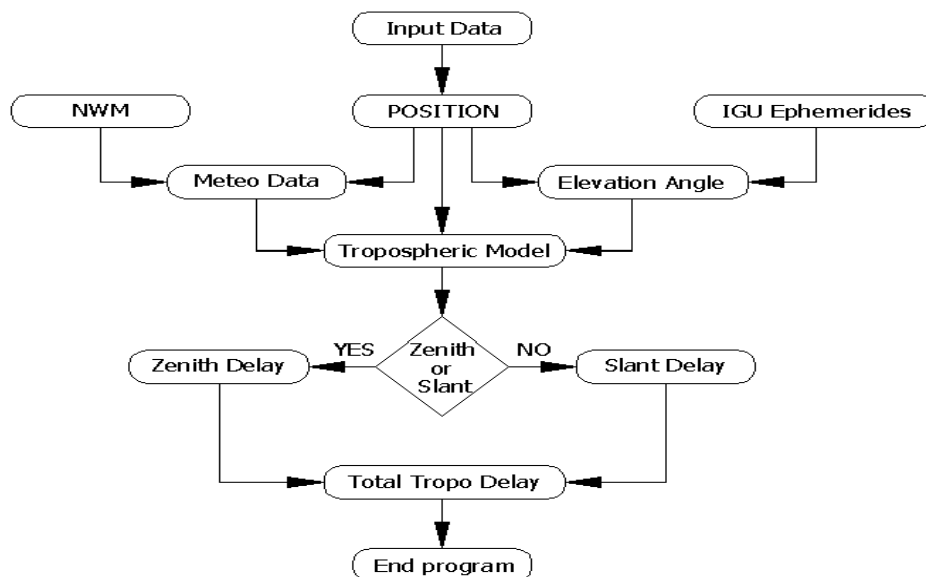


Fig. 3: Main steps of the software implementation

Observing Fig. 3 one can see that the user has to introduce the location of the observation site. The meteorological data are extracted from NWM model according with the geocentric latitude and the orthometric height of the observation site. If only zenith delay is concerned, then the meteorological values are directly used in the standard tropospheric model to compute both non-hydrostatic and wet contribution of the delay, and finally the total zenith tropospheric delay. On the other hand, if the slant path delay is the case, then the elevation angle is computed based on IGU satellite ephemerides and is taken into account by the tropospheric model.

6. Experiments And Analysis

The observation station was chosen the permanent GPS reference station located at Metsähovi, Kirkkonummi (40km east from Helsinki). Data were downloaded as archive files from NOAA's ftp-server¹ for four different days of the year 2006: January 1st, March 20th, June 15th, and September 25th.

Table 1: The location of observation site METS

Station ID	Geodetic coordinates		
	Latitude	Longitude	Height
METS	60°13'03.0"	24°41'43.1"	94.6 m

The International GNSS Service (IGS) *final tropospheric zenith delays*² were used as the reference values in the assessment. The IGS zenith delays were produced with an interval of 2 hours, accuracy of 4 mm, and latency of 4 weeks.

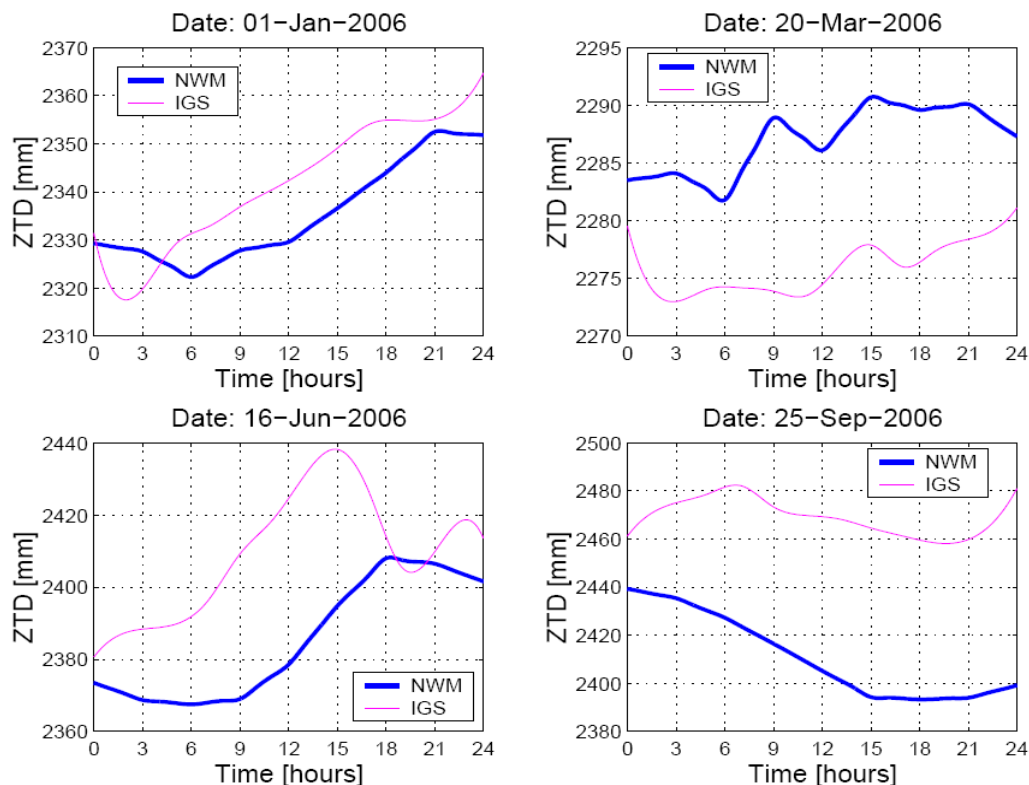


Fig. 4: Comparison of zenith tropospheric delays derived from NWM and the final values produced by IGS for the station METS- Finland.

¹ <ftp://www.arl.noaa.gov/pub/archives/gdas1>

² <http://igscb.jpl.nasa.gov/components/prods.html>

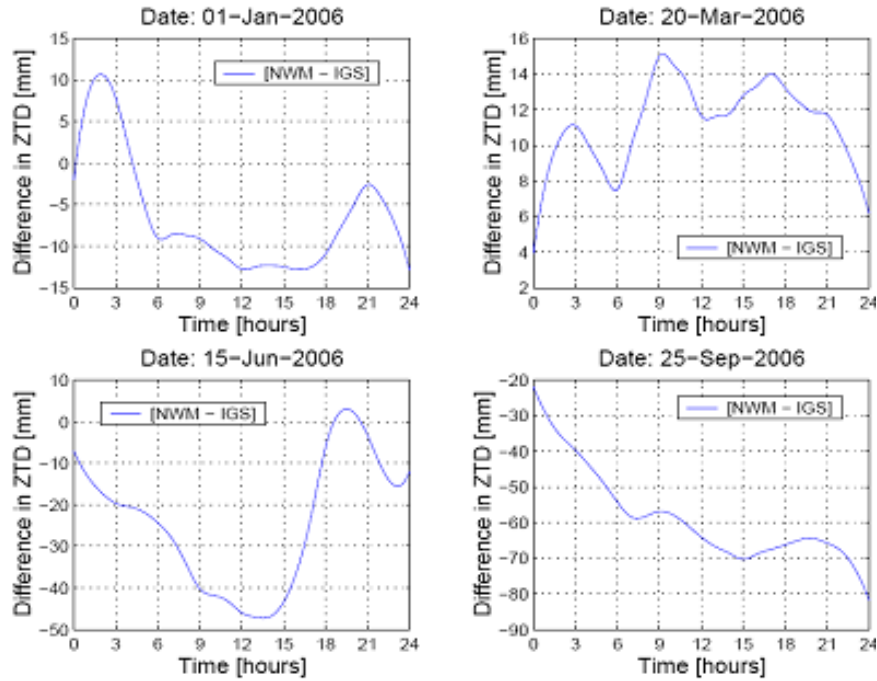


Fig. 5: Difference in zenith tropospheric delay between the NWM-derived estimates and IGS products at the IGS station METS, Finland

Fig. 5 shows the difference between zenith total delays (ZTD) determined using NWM approach and IGS products. The difference between the NWM-derived and IGS-based zenith total delays has a mean that varies in the range between -5.9 cm (September 25th) and $+1.1$ cm (March 20th). These results were obtained using 12 instances in time per the specific day. The mean is significant and indicates a bias between the two different types of zenith delays. However, this has not been investigated any further in connection with this work. On September 25th, the RMS represents 6.0 cm that looks different from the values of other seasons. A summary of the statistics for all four cases is given in Table 2.

Table 2: Mean, standard deviation and RMS of the difference between NWM-derived and IGS-based zenith total delays

Nr. test	Date	Statistics [NWM-IGS]				
		Min [cm]	Max [cm]	Mean [cm]	Std. [cm]	RMS [cm]
1	January 1 st	0.8	-1.2	-0.6	0.7	0.9
2	March 20 th	1.5	0.8	1.1	0.2	1.2
3	June 15 th	0.2	-4.7	-2.5	1.6	2.9
4	September 25 th	-3.0	-7.3	-5.9	1.3	6.0

In order to determine the total delay for satellite signal at any elevation angles, the hydrostatic and wet mapping functions given by Ifadis can be applied to the hydrostatic and wet zenith delays determined from GDAS-model.

7. Conclusions And Future Work

This paper described a way for estimating the tropospheric delay based on numerical weather models. The test results indicate that the NWM-derived tropospheric zenith delays are close to the final tropospheric zenith delays produced by IGS, the accuracy is within 5 cm. This is a good

result considering that IGS products are released with a latency of 4 weeks while NWM provides real-time estimates. Moreover, given the fact that the numerical weather model used has only a medium resolution of $1^{\circ} \times 1^{\circ}$, these numbers are promising, especially for those applications that require a real-time navigation solution. The combination with GPS data is expected to reduce systematic errors and leads to an improved solution. On the other hand, a NWM with a higher resolution could also represent a way to obtain a better accuracy.

As a future work, NWM-based algorithm for estimating tropospheric delays will be integrated with an ionosphere model in order to correct the satellite signal for atmospheric effects in real-time navigation solution. Further studies should be carried out to investigate how this approach affects the final position accuracy especially in real-time applications.

Acknowledgements

The first author is grateful to the Finnish Geodetic Institute for the financial and technical supports offered in pursuing his doctoral research in Finland.

References

1. Brunner, F.K and Welsh, W.M. (1993). *Effects of the troposphere on GPS Measurements*. *GPS World* 4(1):42-51.
2. Herring, T.A. (1992), *Modelling atmospheric delays in the analysis of space geodetic data*, in *Refraction of transatmospheric signals in geodesy*, pp. 157–164.
3. Hofmann-Wellenhof B., Lichtenegger H., Collins J. (2004), *GPS – Theory and Practise*, 5th edition, Springer Wien, NewYork, ISBN 3-211-83534-2.
4. Holton, J.R. (1992). *An Introduction to Dynamic Meteorology*. *International Geophysics Series*, Academic Press. 3rd edition.
5. Jensen, A.B.O. (2002), *Numerical Weather Predictions for Network RTK*. *Publication Series 4*, volume 10, National Survey and Cadastre – Denmark.
6. Kleijer, F. (2004). *Troposphere delay modelling and filtering for precise GPS levelling*, Ph.D thesis, *Mathematical Geodesy and Positioning*, Delft University of Technology.
7. Langley, R.B. (1993), *The GPS Observables*, *GPS World*, April 1993, pp.52-59.
8. Le A.Q., Tiberius C. (2007), *Single-frequency precise point positioning with optimal filtering*. *GPS Solution* 11:61-69.
9. Mendes, V.B. and R.B. Langley (1998). *Tropospheric zenith delay prediction accuracy for airborne GPS high-precision Positioning*. *Proceedings of The Institute of Navigation 54th Annual Meeting*, Denver, CO, U.S.A., 1-3 June; pp. 337-347.
10. Niell, A.E. (1996), *Global mapping functions for the atmosphere delay at radio wavelengths*, *Journal of Geophysical Research (B)*, 101, 3227–3246.
11. Mendes, V.B. (1999), *Modeling the neutral-atmosphere propagation delay in radiometric space techniques*, Ph.D. dissertation, University of New Brunswick.
12. Schueler, T. (2001). *On Ground-based GPS Tropospheric Delay Estimation*. PhD thesis, Universität der Bundeswehr, Munchen.
13. Saastamoinen, J. (1973), *Contributions to the theory of atmospheric refraction*, *Bulletin Geodesique No. 105-107*, pp. 279–298; 383–397; 13–34.
14. Spilker, J.J (1996), *Tropospheric Effects on GPS*, in: *Spilker and Parkinson (eds.), GPS Theory and Applications*, Vol. I, *Progress in Astronautics and Aeronautics*, Vol. 163, pp.517-546.